Separation of optical Kerr and free-carrier nonlinear responses with femtosecond light pulses in $LiNbO_3$ crystals

P. Reckenthaeler, D. Maxein, Th. Woike, and K. Buse
Institute of Physics, University of Bonn, Wegelerstraße 8, D-53115 Bonn, Germany

B. Sturman
Institute of Automation and Electrometry, 630090 Novosibirsk, Russia

(Received 20 December 2006; revised manuscript received 12 April 2007; published 19 November 2007)

Time-resolved four-wave pump-probe experiments with femtosecond light pulses, including readout of the fundamental K grating and also of the $2K$ grating, allow to separate the free-carrier nonlinearity caused by two-photon excitation from the instantaneous optical Kerr nonlinearity. The method is applicable to wide-gap optical materials. For lithium niobate crystals, we show, using 200 fs pulses, that the buildup of the free-carrier grating adiabatically follows the absorbed energy. This finding and the results of modeling lead us to the conclusion that the relaxation (thermalization) time of the photoexcited band carriers is shorter than 100 fs.

DOI: 10.1103/PhysRevB.76.195117 PACS number(s): 42.50.Gy, 77.84.Dy, 78.20.Bh, 78.47.+p

I. INTRODUCTION

Combination of ultrashort durations, high intensities, and moderate energies makes femtosecond light pulses an indispensable tool in the studies of carrier and phonon dynamics in solids.[1–4] Apart from fundamental interest, the "driving force" of these studies is the need for faster devices and faster information processing.

Recently, we employed femtosecond pulses to investigate the nonlinear response of lithium niobate ($LiNbO_3$) crystals,[5–8] a wide-gap material of prime importance for numerous optical applications.[9,10] Using two interfering pump pulses at 388 nm to generate a spatial grating and a weak Bragg-matched pulse at 776 nm to test it, we measured the diffraction efficiency η as a function of the delay time Δt between pump and probe.[7,8] It is characterized by a strong peak at $\Delta t=0$ followed by a quasipermanent (on the picosecond to nanosecond scales) plateau. The peak is caused by an instantaneous χ^3 nonlinearity [the Kerr effect and two-photon absorption (TPA)], while the plateau is of a different nature (it is due to the excitation of free carriers). Similar features are inherent in a number of wide-gap optical materials.[11,12]

The presence of the superimposing peak strongly hampers time-resolved measurements and analysis of light-induced charge excitation and transport on the femtosecond time scale. On the other hand, practically nothing is known here about such fundamental issues as the relaxation times and transport lengths of hot carriers. In particular, they are believed to be closely related to one of the distinctive and important features of lithium niobate crystals—the presence of anomalously strong bulk photovoltaic effect with light-induced fields $\gtrsim 10^5$ V/cm.[13,14] The level of understanding of fast electron phenomena is essentially and unjustifiably lower here compared to that typical of semiconductors such as Si, Ge, and GaAs.

In this paper, we present a general method of how to separate the instantaneous and quasipermanent contributions to the nonlinear response. Furthermore, we report the results of time-resolved measurements and modeling of the buildup of free-carrier gratings in $LiNbO_3$ crystals.

The underlying idea is pretty simple: Two pump pulses form a sinusoidal intensity grating; its grating vector **K** is the difference of the pump wave vectors (see also Fig. 1). In the case of an instantaneous χ^3 nonlinearity, the change of the optical permittivity $\Delta\varepsilon(\mathbf{r},t)$ is proportional to the pump intensity $I_p(\mathbf{r},t)$. Therefore, $\Delta\varepsilon$ is modulated *only* with the spatial frequency K. The quasipermanent free-carrier response, caused by two-photon excitation of electrons, is of a higher order in I_p; it includes not only a K but also a $2K$ spatial frequency component. By Bragg matching a probe beam to the $2K$ grating, one can monitor the net buildup of the free-carrier grating.

II. EXPERIMENTAL METHODS AND RESULTS

Our experimental setup is sketched in Fig. 1. Two identical pump pulses at wavelength $\lambda_p=388$ nm with a temporal full width at half maximum (FWHM) of ≈ 215 fs for the intensities are incident simultaneously and symmetrically onto the YZ face of a $LiNbO_3$ sample, whose thickness is $d=70$ μm. The pump half-angle $\theta_p=4°$ corresponds to the grating period $\Lambda=2\pi/K\simeq 2.8$ μm; the grating vector **K** is chosen to be perpendicular to the polar c axis (i.e., to the z

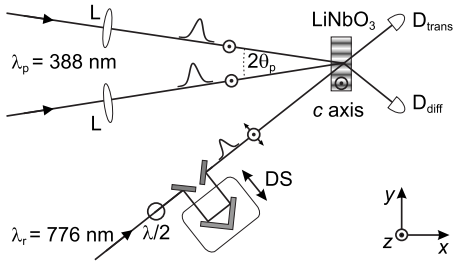

FIG. 1. Schematic presentation of a four-wave pump-probe experiment. D_{diff} and D_{trans} are photodiodes, DS is a delay stage, L is a long-focus lens, and c is the polar axis. The lines inside the sample show schematically the light interference pattern of the pump pulses.

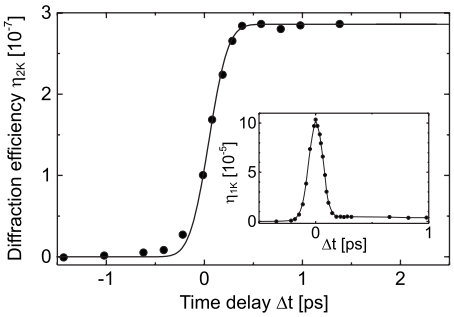

FIG. 2. Diffraction efficiency η_{2K} versus the delay time Δt for the $2K$ grating recorded with $\approx 40\ \mathrm{GW/cm^2}$ pump pulses. The pump and probe pulses are z polarized. The dots are experimental data, and the solid line is the result of calculations. The inset shows a dependence $\eta_{1K}(\Delta t)$ for the $1K$ grating; the solid line is a guide for the eye.

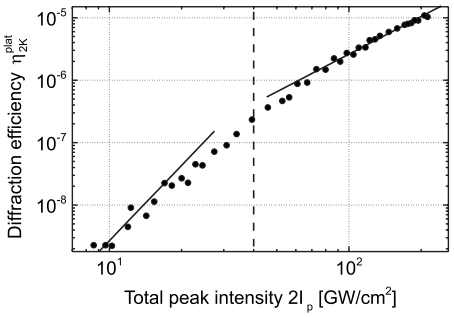

FIG. 3. Intensity dependence of $\eta_{2K}^{\mathrm{plat}}$. The dots refer to the z-z polarization state for the pump-probe pulses. The solid lines are dependences $\eta_{2K}^{\mathrm{plat}} \propto I_p^4$ and I_p^2 in the low- and high-intensity regions. The dashed vertical line at $2I_p = 40\ \mathrm{GW/cm^2}$ separates these regions.

axis). The pump polarization vector is parallel to the z axis (the extraordinary waves).

The FWHM diameter of the pump beams inside the sample, ≈ 0.7 mm, exceeds considerably the grating period. The peak intensity I_p of each pump pulse ranges from ≈ 4 to $\approx 140\ \mathrm{GW/cm^2}$. The grating is probed with a weak pulse at $\lambda_r = 2\lambda_p = 776$ nm, which is Bragg matched either to the $1K$ or to the $2K$ grating; the angle of incidence θ_r being $\approx 8°$ or $\approx 16°$, respectively. Its FWHM duration and diameter are ≈ 165 fs and 3.5 mm. The probe pulse is polarized either along the z axis or along the y axis. Using a delay stage (DS), the delay time Δt between the probe and pump pulses can be varied in the picosecond time range with a resolution of ≈ 10 fs. The main observable characteristic is the diffraction efficiency $\eta = \mathcal{E}_d/(\mathcal{E}_d + \mathcal{E}_t)$, where $\mathcal{E}_d$ and $\mathcal{E}_t$ are the energies of the diffracted and transmitted probe pulses, respectively. These energies were measured by the Si photodiodes $\mathrm{D_{diff}}$ and $\mathrm{D_{trans}}$ (Thorlabs, DET210). The UV light was suppressed using absorptive low pass filters.

The dots in Fig. 2 are our experimental data for $\eta_{2K}(\Delta t)$ obtained for $I_p \approx 40\ \mathrm{GW/cm^2}$. Each dot is the result of averaging over ≈ 100 measurements with a repetition rate of ≈ 10 Hz. The maximum statistical dispersion of the dots, which corresponds to the plateau region, is (10–15)%.

One sees that the diffraction efficiency of the $2K$ grating grows monotonically with Δt and arrives at the plateau value $\eta_{\mathrm{plat}} \approx 3 \times 10^{-7}$. The rise time is comparable with the pulse width. This transient behavior contrasts with that of the $1K$ grating (see the inset of Fig. 2). The latter is characterized by a strong peak at $\Delta t = 0$, caused by the Kerr and TPA effects. The plateau value of η decays only on the nanosecond time scale.[6] We have found also that the dependences $\eta_{1K}(\Delta t)$ and $\eta_{2K}(\Delta t)$ are rather insensitive (within a factor of ≈ 1.5) to the mutual polarization of the pump and probe pulses.

Next, we analyze the dependence of the plateau diffraction efficiency $\eta_{2K}^{\mathrm{plat}}$ on the total peak intensity of the pump pulses, $2I_p$. The experimental results are presented in Fig. 3 on a logarithmic scale. The dots correspond to the z-z polarization combination for the pump-probe pulses. Each point is the result of averaging over ≈ 400 measurements at a repetition rate of 10 Hz. Within the experimental accuracy, the same dependence $\eta_{2K}^{\mathrm{plat}}(2I_p)$ occurs for the z-y polarization state.

One sees that the intensity range consists of low- and high-intensity regions, where the two-photon absorption is weak and strong, respectively.[6,7] The turning point is $2I_p = (\beta_p d)^{-1} \approx 40\ \mathrm{GW/cm^2}$, where $\beta_p \simeq 3.5$ cm/GW is the TPA coefficient at 388 nm. The solid lines in Fig. 3 represent the dependence $\eta_{2K}^{\mathrm{plat}} \propto (2I_p)^b$ in the low- and high-intensity regions with the exponent $b = 4$ and 2, respectively. The dependence $\eta_{2K}^{\mathrm{plat}} \propto I_p^4$ in the low-intensity range indicates a two-photon mechanism for the excitation of free carriers. Here, the pump-induced change of the optical permittivity and the amplitude of the diffracted probe pulse are both proportional to I_p^2, and the energy of the diffracted probe pulse is proportional to I_p^4. A noticeably weaker growth of $\eta_{2K}^{\mathrm{plat}}(I_p)$ in the high-intensity region is due to the nonlinear TPA attenuation of the pump pulses.

III. MODELING

Now we turn to modeling of the observed phenomena. It incorporates several key points as follows (see also Ref. 8):

- Since the temporal FWHMs of the pulses are much larger than the light periods $\lambda_{p,r}/c$, the envelope approximation holds true.
- The spatial lengths of the pulses are smaller than the crystal thickness so that the effects of spatiotemporal overlap are crucial. It is necessary thus to solve the $(3+1)D$ coupled-wave equations.
- The smallness of η allows us to use a perturbation approach to solve the coupled-wave equations.
- The paraxial approximation, exploiting the smallness of the propagation angles in the sample, holds true.
- The spatiotemporal profiles of incident pulses are Gaussian.
- The rate of the nonlinear change of the optical permittivity, $\partial \Delta\varepsilon/\partial t$, which is caused by the two-photon excitation of free carriers, is proportional to $I_p^2(\mathbf{r}, t)$. Recombination processes for photoexcited carriers are negligible on the picosecond time scale.
- The influence of the high-order instantaneous χ^5 nonlinearity is negligible with a big margin of safety.

Within the above assumptions, the dependence $\eta_{2K}(\Delta t)/\eta_{2K}^{\mathrm{plat}}$ can be calculated without any fit parameters. It is determined only by the experimental angular and pulse-width parameters. The final result reads

$$\frac{\eta_{2K}(\Delta t)}{\eta_{2K}^{\mathrm{plat}}} = \frac{a}{4\sqrt{\pi}} \int_{-\infty}^{\infty} \exp\left[-a^2\left(s - \frac{2\Delta t}{w}\right)^2\right][1+\mathrm{erf}(\sqrt{2}s)]^2 ds, \tag{1}$$

where s is the integration variable, w is the Gaussian pulse duration, $\mathrm{erf}(x)$ is the error function, $a = \sqrt{(1+4q^2)/(1+40q^2)}$, $q=\theta_p D/cw$ is a dimensionless angular parameter, $D=D_r/\sqrt{1+4D_r^2/D_p^2}$ is an effective diameter, D_p and D_r are the Gaussian diameters of the pump and readout beams, and c is the speed of light. To calculate the FWHM parameters, it is sufficient to multiply w and $D_{p,r}$ by a factor of $\sqrt{\ln 2} \simeq 0.83$.

The solid line in Fig. 2 is plotted with this relation and the above specified experimental parameters without any fit. It is in very good agreement with the experimental data. With an accuracy better than 100 fs, we can exclude any additional broadening mechanisms.

The calculated plateau value of the diffraction efficiency for the $2K$ grating, $\eta_{2K}^{\mathrm{plat}}$, is $\approx$16 times smaller for the experimental conditions than η_K^{plat} [mostly because of a four times smaller modulation depth of $I_p^2(\mathbf{r})$ at the spatial frequency $2K$]. This prediction is also in good agreement with the data of Fig. 2.

IV. DISCUSSION

Now we discuss the impact of our findings on the notion of charge transfer and transport phenomena in $LiNbO_3$ crystals. It is well known that this wide-gap material possesses a rather weak photoconductivity and an anomalously strong bulk photovoltaic effect (light-induced fields $\gtrsim 10^5$ V/cm). These effects are attributed usually to the thermalized and nonthermalized (hot) charge carriers, respectively.[14,15] The only known explanation of the anomalously high light-induced fields relies on a hypothesis of an extremely short ($<$100 fs) relaxation and/or thermalization of hot electrons to the bottom of the conduction band and shallow energy levels.[14] This relaxation is caused by the electron-phonon coupling, which is expected to be strong in ionic oxide crystals like lithium niobate. It is known also from many experiments, see, e.g., Refs. 8 and 16, that the lifetime (or recombination time) of the thermalized carriers belongs the nanosecond range.

If the relaxation time of photoexcited hot carriers lied in the range of 10^{-1}–10^2 ps, the corresponding temporal features in the $2K$ response would have to be seen. Otherwise, one should suggest that the optical response of free carriers at 776 nm is the same for delocalized hot states and localized thermalized states within an energy range of $\approx$1 eV. Such a suggestion looks nonrealistic for any bearable band model. Furthermore, it would not be in line with the pronounced wavelength dependence of the light absorption of thermalized carriers excited by long pulses.[17]

However, the buildup of free-carrier gratings with 200 fs light pulses shows no such features on the scale of 0.1–10 ps. The only visible possibility to explain it is to accept that thermalization of hot carriers occurs faster than 0.1 ps. It is just employed in our model, where the grating buildup follows adiabatically the absorbed energy. The decay of free-carrier response on the nanosecond scale is due to the recombination of thermalized carriers; it cannot be prescribed to hot carriers. We have thus a strong evidence for fast ($\lesssim$100 fs) intraband processes in lithium niobate (including relaxation to shallow levels). This behavior differs from that typical of semiconductors, where the hot relaxation and/or thermalization time is usually in the range $\gtrsim$1 ps,[1,3,18] although examples of ultrafast energy relaxation ($\approx$0.1 ps) are known even for semiconductors, see, e.g., Ref. 19. To the best of our knowledge, the hot carrier dynamics in wide-gap optical materials, such as lithium niobate crystals, remains virtually unexplored.

Presumably, the formation of the quasipermanent component of the nonlinear response occurs as follows: Strong pump pulses excite electrons from the valence to the conduction band via two-photon absorption. Then the photoexcited carriers relax quickly ($\lesssim$100 fs) to shallow levels or to polaronic states and contribute in this way to the nonlinear permittivity at λ_r=776 nm. This scenario is consistent with the observations of long lasting infrared absorption[16] and strong photovoltaic fields.

It is not excluded that processes of charge separation can contribute in general to the quasipermanent nonlinear response via the linear electro-optic effect. However, these processes have been suppressed in our configuration by aligning the grating vector perpendicular to the c axis.

V. CONCLUSIONS

In conclusion, we have developed a method of how to separate the process of charge excitation via two-photon absorption from instantaneous changes of the optical permittivity. It is shown with $\approx$200 fs light pulses that for lithium niobate crystals, the TPA-initiated buildup of free-charge gratings follows adiabatically the absorbed energy and shows no features of hot-electron relaxation. The characteristic time of the latter should be smaller than 100 fs.

ACKNOWLEDGMENTS

The authors are grateful to O. Beyer for fruitful discussions. Financial support from the Deutsche Forschungsgemeinschaft (Project No. BU913/13) and from the Deutsche Telekom AG is gratefully acknowledged.

[1] A. Othonos, J. Appl. Phys. **83**, 1789 (1998).
[2] A. Dragonmir, J. G. Mclnerney, and D. N. Nikogosyan, Appl. Opt. **41**, 4365 (2002).
[3] T. Sjodin, H. Petek, and H. L. Dai, Phys. Rev. Lett. **81**, 5664 (1998).
[4] A. McClelland, V. Fomenko, and E. Borguet, J. Phys. Chem. B **108**, 3789 (2004).
[5] O. Beyer, D. Maxein, K. Buse, B. Sturman, H. T. Hsieh, and D. Psaltis, Opt. Lett. **30**, 1366 (2005).
[6] O. Beyer, D. Maxein, K. Buse, B. Sturman, H. T. Hsieh, and D. Psaltis, Phys. Rev. E **71**, 056603 (2005).
[7] H. T. Hsieh, D. Psaltis, O. Beyer, D. Maxein, C. von Korff Schmising, K. Buse, and B. Sturman, Opt. Lett. **30**, 2233 (2005).
[8] O. Beyer, D. Maxein, K. Buse, and B. Sturman, J. Opt. Soc. Am. B **24**, 3 (2007).
[9] *Holographic Data Storage*, edited by H. J. Coufal, D. Psaltis, and G. T. Sincerbox (Springer, New York, 2000).
[10] L. E. Myers, R. C. Eckardt, M. M. Fejer, R. L. Byer, W. R. Bosenberg, and J. R. Pierce, J. Opt. Soc. Am. B **12**, 2102 (1995).
[11] T. Sugiyama, H. Fujiwara, T. Suzuki, and K. Tanimura, Phys. Rev. B **54**, 15109 (1996).
[12] P. Martin, S. Guizard, Ph. Daguzan, G. Petite, P. D'Oliveira, P. Meynadier, and M. Perdrix, Phys. Rev. B **55**, 5799 (1997).
[13] A. M. Glass, D. von der Linde, and T. J. Negran, Appl. Phys. Lett. **25**, 233 (1974).
[14] B. I. Sturman and V. M. Fridkin, *The Photovoltaic and Photorefractive Effects in Noncentrosymmetric Materials* (Gordon and Breach, Philadelphia, 1992).
[15] K. Buse, Appl. Phys. B: Lasers Opt. **64**, 391 (1997).
[16] D. Berben, K. Buse, S. Wevering, P. Herth, M. Imlau, and Th. Woike, J. Appl. Phys. **87**, 1034 (2000).
[17] P. Herth, D. Schaniel, Th. Woike, T. Granzow, M. Imlau, and E. Krätzig, Phys. Rev. B **71**, 125128 (2005).
[18] K. Seeger, *Semiconductor Physics* (Springer, New York, 1997).
[19] J. R. Goldman and J. A. Prybyla, Phys. Rev. Lett. **72**, 1364 (1994).